Appl. Chem. Eng., Vol. 32, No. 1, February 2021, 110-116
https://doi.org/10.14478/ace.2020.1109

Article

표면 개질된 나노피브릴화 셀룰로오스를 이용한 에멀젼 안정화 및 고분자 입자 제조

김보영 · 문지연* · 유명재 · 김선민* · 김정아 · 양현승†

한국전자기술연구원 융복합전자소재연구센터, *한국전자기술연구원 나노융합연구센터
(2020년 12월 23일 접수, 2021년 1월 18일 심사, 2021년 1월 19일 채택)

Surface-modified Cellulose Nanofibril Surfactants for Stabilizing Oil-in-Water Emulsions and Producing Polymeric Particles

Bo-Young Kim, Jiyeon Moon*, Myong Jae Yoo, Seonmin Kim*, Jeongah Kim and Hyunseung Yang†

Electronic Convergence Materials & Device Research Center, Korea Electronics Technology Institute, Gyeonggi-do 13509, Republic of Korea
**Nano Materials & Component Research Center, Korea Electronics Technology Institute, Gyeonggi-do 13509, Republic of Korea*
(Received December 23, 2020; Revised January 18, 2021; Accepted January 19, 2021)

Abstract

In this work, the surface of hydrophilic cellulose nanofibrils (CNFs) was modified precisely by varying amounts of cetyltrimethylammonium bromide (CTAB) to produce CNF-based particle surfactants. We found that a critical CTAB density was required to generate amphiphilic CTAB-grafted CNF (CNF-CTAB). Compared to pristine CNF, CNF-CTAB was highly efficient at stabilizing oil-in-water Pickering emulsions. To evaluate their effectiveness as particle surfactants, the surface coverage of oil-in-water emulsion droplets was determined by changing the CNF-CTAB concentration in the aqueous phase. Furthermore, styrene-in-water stabilized by CNF-CTAB surfactants was thermally polymerized to produce CNF-stabilized polystyrene (PS) particles, offering a great potential for various applications including pharmaceuticals, cosmetics, and petrochemicals.

Keywords: *Cellulose, Cellulose nanofibrils, Emulsion, Surface modification, CTAB*

1. Introduction

Pickering emulsion, which was stabilized by solid particles, have attracted increasing attention as alternatives to conventional surfactant-stabilized emulsions[1-3]. In contrast to conventional surfactants, particle surfactants with balanced interfacial wettability are irreversibly adsorbed onto oil/water interfaces, producing extremely stable emulsions[4-6]. Because Pickering emulsions could be especially useful in producing functional templates with unconventional nanostructures such as permeable hollow capsules[7-9], colloidosomes[10,11], and particle-armed polymer latex[12], a variety of colloidal particles including Au[13], SiO_2[14,15], TiO_2[7], iron oxide[16,17], and carbon materials[18] have been investigated to stabilize Pickering emulsions. However, because the demand for environmentally-friendly materials is increasing, particles derived from renewable resources are the most promising candidates for particle-stabilized emulsions.

Cellulose particles derived from natural cellulose sources have been considered for emulsion stabilization due to their renewable and green characteristics and functional oxygen-containing groups on their surface which can be readily modified[19-35]. Among the various types of cellulose and their derivatives, cellulose nanofibrils (CNFs), long and flexible cellulose nano-materials, have received tremendous attention because of their eco-friendly nature, high aspect ratio, mechanical properties, and biodegradability[36-39]. Compared to other cellulose derivatives, the high aspect ratio and flexibility of CNFs allow them to bend at the oil/water interface, increasing their emulsifying ability and long-term stability at low concentrations[24,34,40]. Furthermore, CNF can form web-like network structures at oil/water interfaces, which may protect emulsion droplets from coalescence by acting as a strong steric barrier[21,25]. These distinctive properties extend the range of applications for CNF-stabilized emulsions to polymer particles, gels, and membranes[41]. However, the efficiency of CNFs as surfactants is often limited by the large number of hydrophilic groups, which could impede the modulation of their surface properties in a reproducible and systematic manner. Because particle wettability is generally a critical factor that determines the efficiency of emulsion stabi-

† Corresponding Author: Korea Electronics Technology Institute, Electronic Convergence Materials & Device Research Center, Gyeonggi-do 13509, Republic of Korea
Tel: +82-31-789-7165 e-mail: hsyang@keti.re.kr

pISSN: 1225-0112 eISSN: 2288-4505

lization, an appropriate method for precisely modulating the surface properties of the CNFs must be developed. Several groups have demonstrated that the surface of CNFs can be modified by chemical grafting approaches including silylation and esterification, and CNFs with improved hydrophobicity have been successfully used as efficient surfactants for water-in-oil emulsions[26] and oil-in-water-in-oil double emulsions[28]. However, such approaches typically require multistep reactions and they often suffer from degradation of the unique mechanical properties of CNFs due to the damage to the surfaces of CNF during the chemical grafting process.

In this work, we prepared surface-modified CNF surfactants to stabilize oil-in-water emulsions. The surface of CNFs was modified using cetyltrimethylammonium bromide (CTAB), which has a quaternary ammonium head and long alkyl chains, to produce CTAB-modified CNF (CNF-CTAB) surfactants. With a hydrophilic CNF surface and hydrophobic alkyl chains from the CTAB molecules, the amphiphilic character of the surface-modified CNF will improve the wetting characteristics and alter the position of the CNF to the oil/water interface, thereby enhancing the emulsion stability. We prepared a series of CNF-CTAB formulations with various CTAB densities by controlling the feed ratios of CTAB to the CNF during the surface modification step to investigate the effects of CTAB density on the surface properties and surfactant efficiency of CNF. Compared to the case where strongly hydrophilic CNF-CTAB was used as the surfactant, only amphiphilic CNF-CTAB functioned successfully as a surfactant and stabilized emulsions for up to several months. Furthermore, to demonstrate the potential of amphiphilic CNF-CTAB for producing emulsion-based polymeric materials, we used them in a mini-emulsion polymerization of styrene, and micron-sized, spherical, PS colloidal particles covered with CNF were produced.

2. Experimental Section

2.1. Materials

2,2,6,6-tetramethylpiperidinyl-1-oxyl (TEMPO)-oxidized CNF with average diameter of 13 nm, and lengths of over several micrometers was kindly supplied by Moorim P&P. CTAB, styrene, and ethanol was purchased from Aldrich. Azobisisobutyronitrile (AIBN) was purchased from Junsei and recrystallized from ethanol for purification. Deionized (DI) water was used in all experiments.

2.2. Surface modification of CNF

Before surface modification process, CNF (1 g) were dispersed in ethanol (30 mL), and the mixture was stirred for 24 h vigorously to avoid the presence of aggregated CNF. To prepare surface-modified CNF, CTAB (0.06 g) was added to the mixture. After stirring for 24 h, mixture was centrifuged, and the precipitated product was washed with ethanol and DI water at least 3 times to remove unreacted CTAB completely. For convenience, the product was denoted as CNF-CTAB1. Similar procedures were used to prepare CNF-CTAB0, CNF-CTAB2, CNF-CTAB3, and CNF-CTAB4 with different amount of CTAB, *i.e.*, (0, 0.10, 0.13, 0.15 g), respectively.

2.3. Preparation of Pickering emulsions

All emulsions were prepared using pristine CNF or CNF-CTAB with various CTAB density, where DI water (1 mL) and toluene (1 mL) were used as the aqueous and oil phase, respectively. For all tested emulsions, aqueous phases consisted of CNF-CTAB particles dispersed in water with various concentrations. Oil phase was added afterward. The emulsions were prepared using a homogenizer for 2 min at 20,000 rpm.

2.4. Synthesis of PS particles using mini-emulsion polymerization

By using CNF-CTAB as surfactants, PS particles were prepared by mini-emulsion polymerization following previous reports[18]. Briefly, CNF-CTAB (1 mg), styrene monomer (100 mg), and AIBN (4 mg) were dispersed in DI water (1 mL) and stirred for 20 min. After ultrasonication for 10 min, mixtures were allowed to be polymerized at 70 ℃ for 24 h. Finally, PS particles were purified by repeated centrifugation with ethanol, and finally obtained after drying at room temperature.

2.5. Characterization

FE-SEM (Hitachi S-4800), TEM (ARM-200F, JEOL) were performed to investigate the morphology of pristine CNF, CNF-CTAB, and CNF-stabilized PS particles. Samples of TEM were prepared by dropping suspensions of pristine CNF and CNF-CTAB onto Cu grids coated with carbon film followed by solvent evaporation. Optical microscopy (objective lenses: Mitutoyo M Plan Apo Series, CCD camera: EyeCam) were performed to investigate the morphology of CNF-stabilized emulsions. The image of emulsion droplets was recorded, and the size of droplets was measured using Image J software. Optical photographs of emulsions were taken 24 h after emulsification process to allow the system to be stabilized, and recorded with a digital camera. Grafting of CTAB on the surface of CNF was monitored through fourier-transform infrared spectroscopy (FT-IR) (Nicolet 6700, Thermo) and ζ-potential analyzer (ELSZ-2000, Otsuka Electronics). Thermogravimetry (TGA) (STA-409, Netzsch) was performed to quantify the amount of grafted CTAB on the CNF-CTAB. To observe the change in surface properties of CNF-CTAB, contact angle was measured at least five times using contact angle meter (Phx-300, SEO) with glycerol and diiodomethane as solvents. Samples of contact angle measurements were prepared by drying CNF-CTAB by freeze dryer for 24 h, and dried CNF-CTAB were compressed at 10 MPa to produce CNF-CTAB pellet of 12 mm in diameter and 2 mm in height.

3. Results and Discussion

3.1. Preparation of CNF-CTAB

To tailor the surface properties of hydrophilic CNFs and demonstrate the importance of precisely tuning the surface properties of the CNFs, surface modification of CNFs was conducted. Because CNFs have a negative charge, cationic surfactants such as CTAB strongly interact with their surfaces through electrostatic interactions[42]. A series of CNF-CTAB formulations with different CTAB densities was prepared, which was achieved by simply controlling the feed ratios of CTAB to

Table 1. Characteristics of Various CNF-CTAB used in This Study

	CNF-CTAB0	CNF-CTAB1	CNF-CTAB2	CNF-CTAB3	CNF-CTAB4
Weight loss difference between 200 ℃ and 650 ℃ (%)	94.6	96.6	96.9	97.0	97.2
Grafted CTAB Fraction[a)] (%)	-	2.0	2.3	2.4	2.6

[a)] Calculated from the difference in the weights loss fractions of CNF-CTAB 1,2,3,4 and Pristine CNF (*i.e.* CNF-CTAB0) between 200 ℃ and 650 ℃.

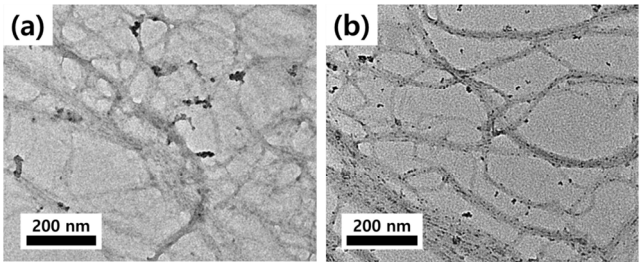

Figure 1. TEM image of (a) pristine CNF and (b) CNF-CTAB3.

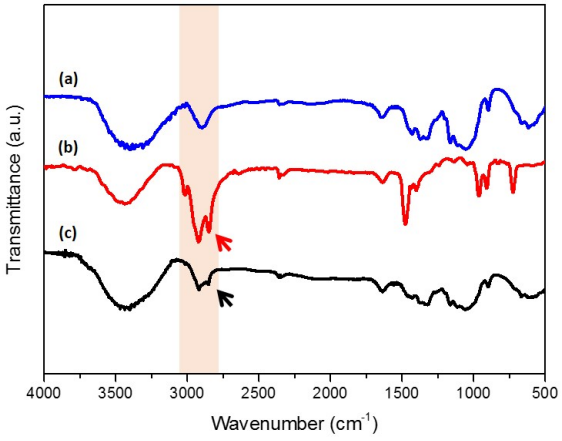

Figure 2. FT-IR spectra of (a) CNF, (b) CTAB, and (c) CNF-CTAB3.

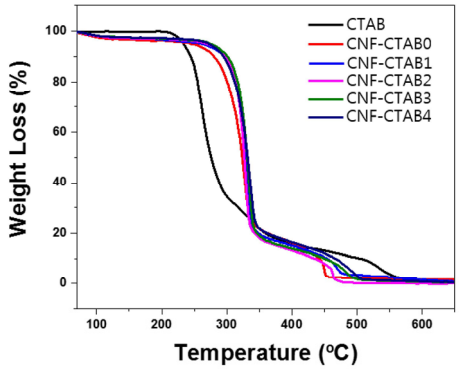

Figure 3. TGA spectra of various CNF-CTAB used in this study.

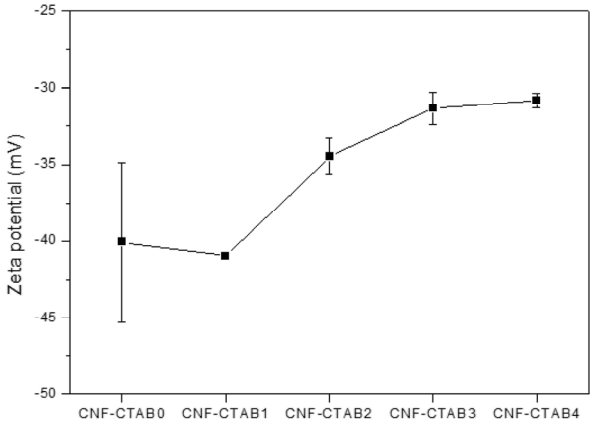

Figure 4. ζ-potential of CNF-CTAB.

CNF during the surface modification step. After surface modification, the CNF-CTAB formulations were well-dispersed in aqueous solvents without aggregation (Figure 1). FT-IR measurements were performed to monitor the grafting of CTAB onto the CNFs (Figure 2). A few important vibration peaks from hydroxyl groups and alkyl chains were monitored and compared. For pristine CNF, a strong peak at 3300 cm^{-1} was observed due to the abundant hydroxyl groups. However, after CTAB modification, CNF-CTAB3 showed new peaks at 2900~2850 cm^{-1} due to the C–H stretching of CTAB molecules. Thus, the CNFs were successfully modified with CTAB molecules. TGA was performed to estimate the amount of CTAB grafted onto the CNF surface through electrostatic interactions (Figure 3, Table 1). Because CTAB was thermally degraded after 200 ℃, the amount of grafted CTAB was assumed based on the weight loss between 200 and 650 ℃. As shown in Table 1, the amount of grafted CTAB in CNF-CTAB1, CNF-CTAB2, CNF-CTAB3, and CNF-CTAB4 was estimated to be 2.0, 2.3, 2.4, and 2.6%. ζ-potential measurements provided additional evidence confirming the grafting of CTAB onto the CNF surface through electrostatic interactions (Figure 4). Whereas CNF-CTAB0 has a negative charge of approximately -40 mV, which is comparable to previous reports[43], the ζ-potential increased as the amount of grafted CTAB molecules increased. These results reveal that electrostatic attraction between the charged sites on CNF and the charged headgroups of CTAB molecules occurs, compensating for the negative CNF charges. Particularly, for the reason of ζ-potential of CNF-CTAB4 was not significantly increased compared to that of CNF-CTAB3, we speculate that CTAB molecules were not sufficiently grafted onto some aggregated-CNF.

We performed contact angle measurements on CNF-CTAB to measure changes in surface energy after CTAB modification. Table 2 summarizes the measured glycerol and diiodomethane contact angles on each CNF-CTAB. Each CNF-CTAB exhibits a different glycerol and diiodomethane contact angle [CNF-CTAB0 (44.8°, 23.9°), CNF-CTAB1 (52.0°, 28.1°), CNF-CTAB2 (63.7°, 31.6°), CNF-CTAB3 (68.1°, 31.3°), and CNF-CTAB4 (60.4°, 26.2°)]. Based on these results, the surface energies of different CNF-CTAB derivatives were determined using the

Table 2. Contact Angle and Calculated Surface Energy of Various CNF-CTAB

	$\theta_{glycerol}$ (°)	$\theta_{diiodomethane}$ (°)	Surface energy (mN/m)
CNF-CTAB0	44.8	23.9	51.1
CNF-CTAB1	52.0	28.1	47.7
CNF-CTAB2	63.7	31.6	43.9
CNF-CTAB3	68.1	31.3	43.6
CNF-CTAB4	60.4	26.2	46.2

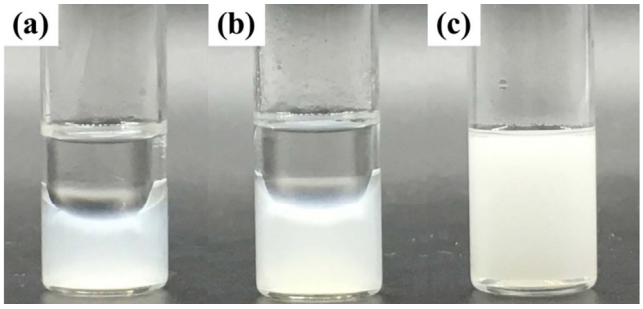

Figure 5. Photographic images of Pickering emulsions stabilized by (a) CNF-CTAB0, (b) CNF-CTAB1, and (c) CNF-CTAB3 at constant concentration of 1.0 mg/mL.

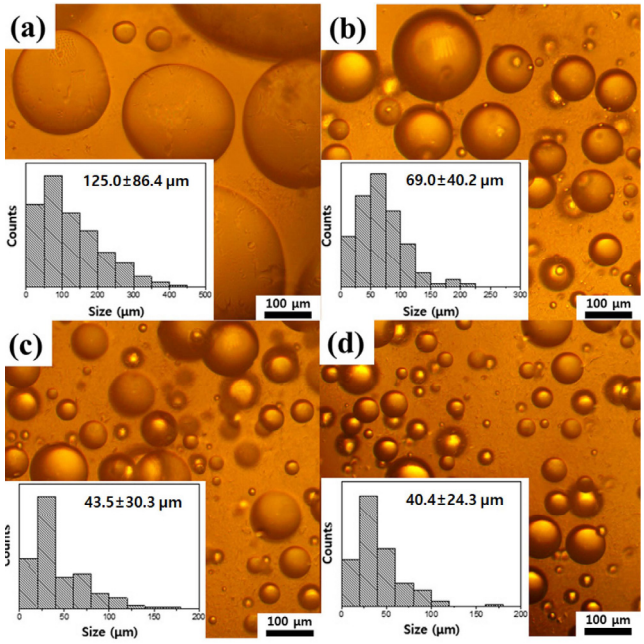

Figure 6. Optical microscopic images of toluene-in-water Pickering emulsions stabilized by CNF-CTAB3 with various concentration: (a) 0.2 mg/mL, (b) 0.5 mg/mL, (c) 1.0 mg/mL, (d) 3.0 mg/mL. The inset is a histogram of the size distribution of the emulsion droplets.

Owens-Wendt method[44]. The surface energy had a decreased as a function of grafted CTAB density, *i.e.*, 51.1 (CNF-CTAB0), 47.7 (CNF-CTAB1), 43.9 (CNF-CTAB2), and 43.6 mN/m (CNF-CTAB3), indicating that the density of hydrophobic alkyl chains gradually increased. However, the surface energy of CNF-CTAB4, which has more grafted-CTAB molecules than CNF-CTAB3, increased to 46.2 mN/m. It is noteworthy that CTAB itself can form bilayers as a result of hydrophobic interactions between their hydrocarbon tails. As the number of CTAB molecules participating the surface modification process increases, we speculate that some CTAB molecules may form bilayer structures on the CNF surface through hydrophobic interactions between CTAB molecules[28,45]. Furthermore, the ionic headgroups of CTAB molecules are exposed to the outside, thus leading to a slight increase in the hyrdophilicity and surface energy of the CNF-CTAB4.

3.2. Pickering emulsion stabilized by CNF-CTAB

In order to investigate the ability of the surface-modified CNF-CTAB formulations to stabilize oil/water emulsions, a series of toluene/water mixtures (1/1 mL) was prepared. The various CNF-CTAB formulations were added to the mixtures and the mixtures were emulsified. As shown in Figure 5, when CNF-CTAB0 or CNF-CTAB1 was added, their strong hydrophilic character hindered their partitioning to the oil/water interface, emulsions were unstable, and phase separation occurred in a few minutes [Figure 5 (a), (b)]. In contrast, the addition of CNF-CTAB3 created dense, white emulsions consisting of micron-sized emulsion droplets that were extremely stable up to several months [Figure 5 (c)]. This clearly indicated that CTAB modification imparts amphiphilicity, promoting the adsorption of CNF onto the toluene/water interface and thus stabilizing the interface.

To investigate the efficiency of the CNF-CTAB3 surfactant, the number-average size of emulsion droplets and their size distribution were obtained by analyzing optical microscopic images (Figure 6). The size of toluene droplets varied based on the concentration of CNF-CTAB3. The droplet size decreased from 125 to 43 μm as the concentration increased from 0.2 to 1.0 mg/mL. This particle concentration dependence is a common feature of Pickering emulsions stabilized by particles. The decrease in the average droplet size was associated with CNF-CTAB3 adsorption at the toluene/water interface. However, once the concentration of CNF-CTAB3 approached 1.0 mg/mL, a further increase in the amount of CNF-CTAB3 did not induce a significant reduction in the droplet size. To evaluate the influence of the concentration of CNF-CTAB3 on the emulsion stability, the surface coverage (*C*) (*i.e.*, the ratio between the maximum surface area of CNF particles to the total surface area of oil droplets), was estimated according to previous literature[21,46]:

$$C\ (\%) = m_p D\ /\ 6w\rho V_{oil} \times 100\% \quad (1)$$

where m_p is the amount of CNF particles dispersed in the aqueous phase, D is the surface-mean diameter of the emulsion droplets, w is the width of the CNF-CTAB3 measured by TEM (13 nm), ρ is the density of CNF-CTAB3 assuming that this density is similar to that of pristine CNF (1.4 g/cm^3)[47], and V_{oil} is the volume of the emulsified oil phase (1 mL). As shown in Table 3, toluene-in-water emulsion droplets were relatively stable to coalescence when only about 22.9% of their surface was covered with CNF-CTAB3. We speculate that this

Table 3. Calculated Interfacial Coverage of CNF-CTAB3 on Oil Droplets

Concentration of CNF-CTAB3	0.2 mg/mL	0.5 mg/mL	1.0 mg/mL	3.0 mg/mL
Diameter of the emulsion droplets (μm)	125.0	69.0	43.5	40.4
Surface coverage (%)	22.9	31.6	39.8	111.0

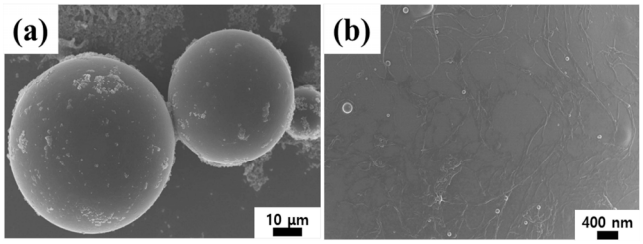

Figure 7. SEM images of (a) polymerized styrene-in-water emulsions stabilized by CNF-CTAB3 and (b) CNF at the surface of PS particles.

occurs because the high aspect ratio of CNF-CTAB3 allows for flexibility when aligned along the droplet interface, forming an entangled network that acts as a strong steric barrier[27,48]. This results in the stabilization of emulsion droplets with a lower surface coverage. When the concentration of CNF-CTAB3 increased to 3.0 mg/mL, the calculated surface coverage values for the oil droplets were greater than 100%. This may have occurred because multilayers were formed at the droplet surfaces due to their ability to bend and overlap at the oil/water interface or because some excess CNF-CTAB3 was in the aqueous phase. At an increased CNF-CTAB3 concentration, a higher interfacial coverage around the oil droplets occurred, reducing the droplet size and leading to more uniform and stable oil droplets.

The practical application of oil-in-water emulsions is the development of particle-stabilized polymer particles used in coatings, cosmetics, and pharmaceuticals. In order to evaluate the use of CNF-CTAB3 for the preparation of polymer particles, styrene-in-water emulsions stabilized by CNF-CTAB3 were thermally polymerized using AIBN as initiator. This Pickering emulsion polymerization of styrene produced spherical, micrometer-sized PS particles [Figure 7(a)]. It should be noted that non-covered, nanometer-sized PS particles were artifactual outgrowths formed during styrene polymerization, which has been previously reported for cellulose-based Pickering emulsions[27,40]. In the case of micrometer-sized PS particles, CNFs are clearly distributed at the surface of PS particles and bent along their curvature, confirming that they are strongly absorbed at the interface [Figure 7(b)].

4. Conclusions

In this work, we prepared CTAB-modified CNFs with tailored surface properties and demonstrated their applicability as efficient surfactants for stabilizing oil-in-water emulsions. By controlling the grafted ratio of CTAB surfactants, the surface properties of CNF-CTAB was precisely tuned as characterized by contact angle measurements and a ζ-potential analyzer. Compared to CNF-CTAB0, which is strongly hydrophilic and leads to excess CNF-CTAB0 in the aqueous phase, amphiphilic CNF-CTAB3 was positioned at the interface between the oil and aqueous phases. CNF-CTAB3 efficiently stabilized toluene-in-water emulsions against coalescence for more than several months. To investigate the surface organization and surface coverage of emulsion droplets stabilized by CNF-CTAB3, emulsions with varying concentrations of CNF-CTAB3 surfactants were characterized using optical microscopy. Furthermore, to demonstrate the potential of CNF-CTAB3 for the preparation of emulsion-based polymer particles, styrene-in-water emulsions were successfully polymerized to form CNF-CTAB3-stabilized PS particles. Our strategy for the modification of CNF by CTAB molecules provides a facile method to produce amphiphilic CNF surfactants for stabilizing Pickering emulsions and fabricating CNF-based polymer particles.

Acknowledgments

This research was financially supported by the Ministry of Trade, Industry and Energy (MOTIE) and Korea Institute for Advancement of Technology (KIAT) through the International Cooperative R&D program. (Grant: N053100013)

References

1. A. D. Dinsmore, M. F. Hsu, M. G. Nikolaides, M. Marquez, A. R. Bausch, and D. A. Weitz, Colloidosomes: Selectively permeable capsules composed of colloidal particles, *Science*, **298**, 1006-1009 (2002).
2. B. P. Binks, Particles as surfactants - Similarities and differences, *Curr. Opin. Colloid Interface Sci.*, **7**, 21-41 (2002).
3. R. Aveyard, B. P. Binks, and J. H. Clint, Emulsions stabilised solely by colloidal particles, *Adv. Colloid Interface Sci.*, **100-102**, 503-546 (2003).
4. K. Stratford, R. Adhikari, I. Pagonabarraga, J. C. Desplat, and M. E. Cates, Chemistry: Colloidal jamming at interfaces: A route to fluid-bicontinuous gels, *Science*, **309**, 2198-2201 (2005).
5. E. Vignati, R. Piazza, and T. P. Lockhart, Pickering emulsions: Interfacial tension, colloidal layer morphology, and trapped-particle motion, *Langmuir*, **19**, 6650-6656 (2003).
6. F. Tu, B.J. Park, and D. Lee, Thermodynamically stable emulsions using Janus dumbbells as colloid surfactants, *Langmuir*, **29**, 12679-12687 (2013).
7. T. Chen, P. J. Colver, and S. A. F. Bon, Organic-inorganic hybrid hollow spheres prepared from TiO_2-stabilized Pickering emulsion polymerization, *Adv. Mater.*, **19**, 2286-2289 (2007).
8. P. Van Rijn, N. C. Mougin, D. Franke, H. Park, and A. Böker, Pickering emulsion templated soft capsules by self-assembling cross-linkable ferritin-polymer conjugates, *Chem. Commun.*, **47**, 8376-8378 (2011).
9. J. Xu, A. Ma, Z. Xu, X. Liu, D. Chu, and H. Xu, Synthesis of Au and Pt hollow capsules with single holes via Pickering emul-

sion strategy, *J. Phys. Chem. C.*, **119**, 28055-28060 (2015).
10. D. Lee and D. A. Weitz, Double emulsion-templated nanoparticle colloidosomes with selective permeability, *Adv. Mater.*, **20**, 3498-3503 (2008).
11. D. Lee and D. A. Weitz, Nonspherical colloidosomes with multiple compartments from double emulsions, *Small*, **5**, 1932-1935 (2009).
12. S. Cauvin, P. J. Colver, and S. A. F. Bon, Pickering stabilized miniemulsion polymerization: Preparation of clay armored latexes, *Macromolecules*, **38**, 7887-7889 (2005).
13. M. Tang, X. Wang, F. Wu, Y. Liu, S. Zhang, X. Pang, X. Li, and H. Qiu, Au nanoparticle/graphene oxide hybrids as stabilizers for Pickering emulsions and Au nanoparticle/graphene oxide@polystyrene microspheres, *Carbon*, **71**, 238-248 (2014).
14. H. Zhou, T. Shi, X. Zhou, Preparation of polystyrene/SiO_2 microsphere via Pickering emulsion polymerization: Synergistic effect of SiO_2 concentrations and initiator sorts, *Appl. Surf. Sci.*, **266**, 33-38 (2013).
15. D. Yin, Q. Zhang, C. Yin, Y. Jia, and H. Zhang, Effect of particle coverage on morphology of SiO_2-covered polymer microspheres by Pickering emulsion polymerization, *Colloids Surfaces A Physicochem. Eng. Asp.*, **367**, 70-75 (2010).
16. K. Y. A. Lin, H. Yang, C. Petit, and W. der Lee, Magnetically controllable Pickering emulsion prepared by a reduced graphene oxide-iron oxide composite, *J. Colloid Interface Sci.*, **438**, 296-305 (2015).
17. J. Zhou, X. Qiao, B.P. Binks, K. Sun, M. Bai, Y. Li, and Y. Liu, Magnetic Pickering emulsions stabilized by Fe_3O_4 nanoparticles, *Langmuir*, **27**, 3308-3316 (2011).
18. H. Yang, D. J. Kang, K. H. Ku, H. H. Cho, C. H. Park, J. Lee, D. C. Lee, P. M. Ajayan, and B. J. Kim, Highly luminescent polymer particles driven by thermally reduced graphene quantum dot surfactants, *ACS Macro Lett.*, **3**, 985-990 (2014).
19. I. Capron, O. J. Rojas, R. Bordes, Behavior of nanocelluloses at interfaces, *Curr. Opin. Colloid Interface Sci.*, **29**, 83-95 (2017).
20. M. Matos, A. Marefati, R. Bordes, G. Gutiérrez, M. Rayner, Combined emulsifying capacity of polysaccharide particles of different size and shape, *Carbohydr. Polym.*, **169**, 127-138 (2017).
21. Y. Goi, S. Fujisawa, T. Saito, K. Yamane, K. Kuroda, and A. Isogai, Dual functions of TEMPO-oxidized cellulose nanofibers in oil-in-water emulsions: A Pickering emulsifier and a unique dispersion stabilizer, *Langmuir*, **35**, 10920-10926 (2019).
22. K. Xhanari, K. Syverud, and P. Stenius, Emulsions stabilized by microfibrillated cellulose: The effect of Hydrophobization, concentration and O/W ratio, *J. Dispers. Sci. Technol.*, **32**, 447-452 (2011).
23. N. Nikfarjam, N. Taheri Qazvini, and Y. Deng, Surfactant free Pickering emulsion polymerization of styrene in w/o/w system using cellulose nanofibrils, *Eur. Polym. J.*, **64**, 179-188 (2015).
24. Z. Hu, S. Ballinger, R. Pelton, and E. D. Cranston, Surfactant-enhanced cellulose nanocrystal Pickering emulsions, *J. Colloid Interface Sci.*, **439**, 139-148 (2015).
25. J. Ojala, M. Visanko, O. Laitinen, M. Österberg, J.A. Sirviö, H. Liimatainen, Emulsion stabilization with functionalized cellulose nanoparticles fabricated using deep eutectic solvents, *Molecules*, **23**, 2765-2782 (2018).
26. M. Andresen and P. Stenius, Water-in-oil emulsions stabilized by hydrophobized microfbrillated cellulose, *J. Dispers. Sci. Technol.*, **28**, 837-844 (2007).
27. I. Kalashnikova, H. Bizot, B. Cathala, and I. Capron, New Pickering emulsions stabilized by bacterial cellulose nanocrystals, *Langmuir*, **27**, 7471-7479 (2011).
28. A. G. Cunha, J. B. Mougel, B. Cathala, L. A. Berglund, and I. Capron, Preparation of double Pickering emulsions stabilized by chemically tailored nanocelluloses, *Langmuir*, **30**, 9327-9335 (2014).
29. I. Kalashnikova, H. Bizot, P. Bertoncini, B. Cathala, and I. Capron, Cellulosic nanorods of various aspect ratios for oil in water Pickering emulsions, *Soft Matter*, **9**, 952-959 (2013).
30. C. Wen, Q. Yuan, H. Liang, and F. Vriesekoop, Preparation and stabilization of d-limonene Pickering emulsions by cellulose nanocrystals, *Carbohydr. Polym.*, **112**, 695-700 (2014).
31. T. Winuprasith and M. Suphantharika, Microfibrillated cellulose from mangosteen (*Garcinia mangostana* L.) rind: Preparation, characterization, and evaluation as an emulsion stabilizer, *Food Hydrocoll.*, **32**, 383-394 (2013).
32. M. Visanko, H. Liimatainen, J.A. Sirviö, J. P. Heiskanen, J. Niinimäki, and O. Hormi, Amphiphilic cellulose nanocrystals from acid-free oxidative treatment: Physicochemical characteristics and use as an oil-water stabilizer, *Biomacromolecules*, 15, 2769-2775 (2014).
33. Y. Zhang, V. Karimkhani, B. T. Makowski, G. Samaranayake, and S. J. Rowan, Nanoemulsions and nanolatexes stabilized by hydrophobically functionalized cellulose nanocrystals, *Macromolecules*, **50**, 6032-6042 (2017).
34. Q. Li, Y. Wang, Y. Wu, K. He, Y. Li, X. Luo, B. Li, C. Wang, and S. Liu, Flexible cellulose nanofibrils as novel Pickering stabilizers: The emulsifying property and packing behavior, *Food Hydrocoll.*, **88**, 180-189 (2019).
35. C. A. Carrillo, T. E. Nypelö, O. J. Rojas, Cellulose nanofibrils for one-step stabilization of multiple emulsions (W/O/W) based on soybean oil, *J. Colloid Interface Sci.*, **445**, 166-173 (2015).
36. D. Klemm, F. Kramer, S. Moritz, T. Lindström, M. Ankerfors, D. Gray, and A. Dorris, Nanocelluloses: A new family of nature-based materials, *Angew. Chemie - Int. Ed.*, **50**, 5438-8466 (2011)
37. N. Lavoine, I. Desloges, A. Dufresne, and J. Bras, Microfibrillated cellulose - Its barrier properties and applications in cellulosic materials: A review, *Carbohydr. Polym.*, **90**, 735-764 (2012).
38. A. Isogai, T. Saito, and H. Fukuzumi, TEMPO-oxidized cellulose nanofibers, *Nanoscale*, **3**, 71-85 (2011).
39. H. P. S. Abdul Khalil, A. H. Bhat, and A. F. Ireana Yusra, Green composites from sustainable cellulose nanofibrils: A review, *Carbohydr. Polym.*, **87**, 963-979 (2012).
40. L. Bai, S. Huan, W. Xiang, L. Liu, Y. Yang, R. W. N. Nugroho, Y. Fan, and O. J. Rojas, Self-assembled networks of short and long chitin nanoparticles for oil/water interfacial superstabilization, *ACS Sustain. Chem. Eng.*, **7**, 6497-6511 (2019).
41. W. Chen, H. Yu, S.Y. Lee, T. Wei, J. Li, and Z. Fan, Nanocellulose: A promising nanomaterial for advanced electrochemical energy storage, *Chem. Soc. Rev.*, **47**, 2837-2872 (2018).
42. S. Alila, S. Boufi, M. N. Belgacem, and D. Beneventi, Adsorption of a cationic surfactant onto cellulosic fibers I. Surface charge effects, *Langmuir*, **21**, 8106-8113 (2005).
43. B. L. Tardy, S. Yokota, M. Ago, W. Xiang, T. Kondo, R. Bordes, and O. J. Rojas, Nanocellulose–surfactant interactions, *Curr. Opin. Colloid Interface Sci.*, **29**, 57-67 (2017).
44. D. K. Owens and R. C. Wendt, Estimation of the surface free energy of polymers, *J. Appl. Polym. Sci.*, **13**, 1741-1747 (1969).
45. E. Y. Bryleva, N. A. Vodolazkaya, N. O. Mchedlov-Petrossyan, L.

V. Samokhina, N. A. Matveevskaya, and A. V. Tolmachev, Interfacial properties of cetyltrimethylammonium-coated SiO_2 nanoparticles in aqueous media as studied by using different indicator dyes, *J. Colloid Interface Sci.*, **316**, 712-722 (2007).
46. C. Tang, S. Spinney, Z. Shi, J. Tang, B. Peng, J. Luo, and K. C. Tam, Amphiphilic cellulose nanocrystals for enhanced Pickering emulsion stabilization, *Langmuir*, **34**, 12897-12905 (2018).
47. H. Fukuzumi, T. Saito, and A. Isogai, Influence of TEMPO-oxidized cellulose nanofibril length on film properties, *Carbohydr. Polym.*, **93**, 172-177 (2013).
48. L. Bai, S. Lv, W. Xiang, S. Huan, D. J. McClements, and O. J. Rojas, Oil-in-water Pickering emulsions via microfluidization with cellulose nanocrystals: 1. Formation and stability, *Food Hydrocoll.*, **96**, 699-708 (2019).

Authors

Bo-Young Kim; M.Sc., Researcher, Electronic Convergence Materials & Device Research Center, Korea Electronics Technology Institute, Seongnam 13509, Korea; kby0827@keti.re.kr

Jiyeon Moon; B.Sc., Researcher, Nano Materials & Component Research Center, Korea Electronics Technology Institute, Seongnam 13509, Korea; letbounce@keti.re.kr

Myong Jae Yoo; Ph.D, Principal Researcher, Electronic Convergence Materials & Device Research Center, Korea Electronics Technology Institute, Seongnam 13509, Korea; jsayoo10@keti.re.kr

Seonmin Kim; Ph.D, Principal Researcher, Nano Materials & Component Research Center, Korea Electronics Technology Institute, Seongnam 13509, Korea; ksunmin@keti.re.kr

Jeongah Kim; B.Sc., Graduate student, Electronic Convergence Materials & Device Research Center, Korea Electronics Technology Institute, Seongnam 13509, Korea; jeongahkim@keti.re.kr

Hyunseung Yang; Ph.D, Senior Researcher, Electronic Convergence Materials & Device Research Center, Korea Electronics Technology Institute, Seongnam 13509, Korea; hsyang@keti.re.kr